Chemical Papers
https://doi.org/10.1007/s11696-021-01685-w

ORIGINAL PAPER

Self-assembly and steric hindrance for further host–guest interactions of a tetrahedral cage $Fe^{II}_4L_4$

Ning Bu[1] · Wen-Yuan Wu[1] · Peng Jiang[1] · Zi-Yuan Zhan[1] · Jin-Long Wan[1] · Zi-Jing Wu[1] · Rong Wan[1]

Received: 17 January 2021 / Accepted: 27 April 2021
© Institute of Chemistry, Slovak Academy of Sciences 2021

Abstract

In this paper, a novel complex $[Fe^{II}_4L_4]^{8+}$ was designed and synthesized from subcomponent self-assembly of C_3-symmetric 2,4,6-tris(4-aminophenoxy)triazine, 3-methylpyridine-2-carboxaldehyde and iron(II) trifluoromethanesulfonate in CH_3CN solution. The structure of target compound was confirmed by ^1H NMR and ESI-MS measurements as a tetrahedral cage, and the host–guest interactions between the complex and a series of guest molecules were studied. The results show that the intermolecular interactions are relatively weak by comparison with other similar ligand's complexes, which may be due to the steric effect of methyl groups adjacent to the peripheral apertures of the cage.

Keywords Cage complex · Self-assembly · Iron(II) · Host–guest interaction

Introduction

Supramolecular compounds have been a topic of great interest in the past several decades due to their diverse characteristics (Cram 1992; Liu et al. 2006; Du et al. 2008; Breniner et al. 2011; Chakrabarty et al. 2011; Schenider et al. 2012). One class of these molecules, hollow cage complexes, has been widely studied for their appealing host–guest properties (Furutani et al. 2009; Gupta et al. 2012). The construction of these complexes is involved in specific geometric shape, three-dimensional configuration and excellent symmetry (Hasenknopf et al. 1996; Caulder and Raymond 1999a; Chichak et al. 2004; Fujita et al. 2005; Bonnet et al. 2006; Sun et al. 2010). These well-defined cage complexes allow for diverse applications, such as gas storage (Riddell et al. 2011), guests separation (Brenner et al. 2017), organic catalysis (Murase et al. 2010; Neelakandan et al. 2015), molecular recognition (Nakabayashi et al. 2008; Clever et al. 2009; Ariga et al. 2012), unstable species protection (Yoshizawa et al. 2005; Horiuchi et al. 2011), fluorescent sensor (Li et al. 2012) and molecular magnet switching (Li et al. 2019). Such elaborate architectures could be amazingly prepared from simple building blocks through the formation of dynamic-covalent (C = N) and coordinative (N → M) bonds during the subcomponent self-assembly process (Ronson et al. 2013; Castilla et al. 2014; Zarra et al. 2015).

Triazine-based ligands featuring C_3-symmetry and other attractive characteristics also have the advantages of flexible synthetic routes, which provide convenience for designing diverse metal–organic constructions, including discrete complexes and framework structures (Yu et al. 2021). In our previous paper (Fu et al. 2018), we reported the development of a helicate complex $[Fe^{II}_2L_3]^{4+}$ through the self-assembly of 4,4′,4″-(1,3,5-triazine-2,4,6-triyl)trianiline, octahedral iron(II) and 2-formyl pyridine (Scheme 1), and found that it could bind electron-rich guest molecules by aromatic π-π interactions.

Herein, we designed and synthesized a novel complex by modifying the subcomponent triazine-trianiline via the insertion of an ether group between triazine and aniline structure (Scheme 2). This modification could improve the flexibility of the ligand for the reason of the free rotation ability of O–C single bond, which allows the ligand more versatile to develop even more complicated metal–organic structures. Then the complex formed by self-assembly was confirmed by NMR and ESI-MS to be a much larger cage structure other than the helicate (Scheme 3). The host–guest relationships between the complex and selected guest molecules were investigated.

✉ Wen-Yuan Wu
wwy@njtech.edu.cn

✉ Rong Wan
rwan@njtech.edu.cn

[1] College of Chemistry and Molecular Engineering, Nanjing Tech University, Nanjing, People's Republic of China

Published online: 07 May 2021

Scheme 1 Self-assembly of the helicate **1**

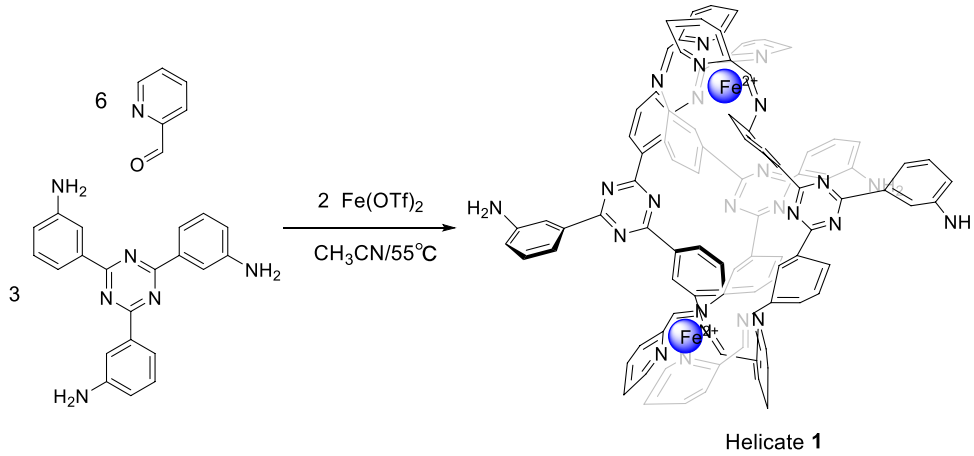

Scheme 2 Synthesis of sub-component triamine

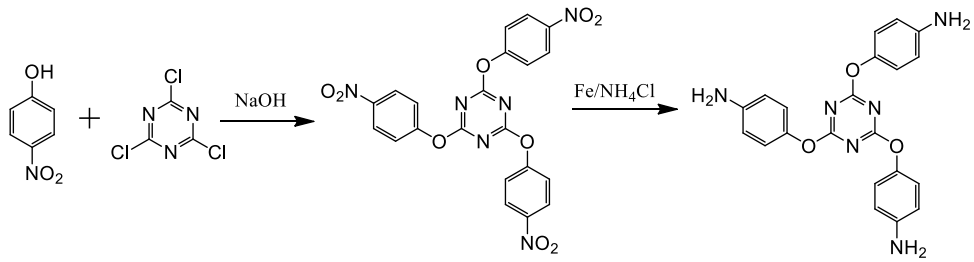

Scheme 3 Self-assembly of tetrahedral cage **1**

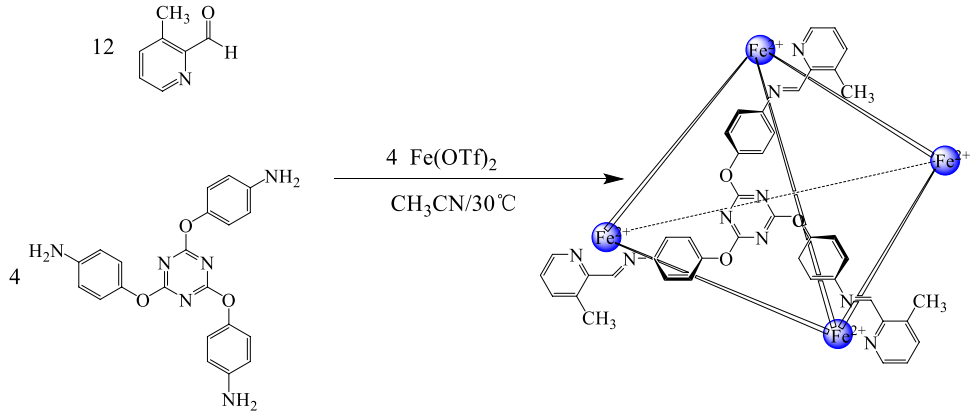

Experimental

Materials and apparatus

All reagents and solvents were purchased from commercial sources and used as supplied except otherwise stated. ^{1}H NMR spectra were recorded on a Bruker Avance DPX400 MHz spectrometer. High-resolution electrospray ionization mass spectrometry (HRMS-ESI) was performed on a Thermo Fisher Scientific Q Exactive device.

Synthesis of the subcomponent triamine

To obtain the subcomponent triamine 2,4,6-tri(4-aminophenoxy)triazine, two steps reactions are needed (Scheme 2).

First, to a stirred solution of cyanuric chloride (1.5 g, 8.2 mmol) in acetone (100 mL) was added slowly a solution of p-nitrophenol (3.00 g, 25.2 mmol) and NaOH (1.00 g, 25.2 mmol) in H_2O (100 mL) and acetone (20 mL) with gentle cooling. The combined solution was heated and stirred under reflux for 2 h under 60 ℃. The crude product was

collected by filtration, washed with H_2O (20 mL) and MeOH (20 mL) for three times, and dried under vacuum to give 2,4,6-tris(4-nitrophenoxy)triazine as white crystalline solid.

Then, to a 250-mL flask, 1.78 g (3.7 mmol) of 2,4,6-tris(4-nitrophenoxy)triazine, 3 g (55 mmol) of ammonium chloride, 60 mL of ethanol and 20 mL of water were added. The mixture was stirred and heated to 80 ℃. Reduced iron powder 3 g (55 mmol) was added and the reaction was continued under refluxed for 2 h. Then the reaction mixture was filtered and the filter cake was washed with hot ethanol 10 mL for twice. The combined filtrate was adjusted to pH 9 with sodium bicarbonate. The crude product was precipitated, filtered and recrystallized from methanol to give pale yellow 2,4,6-tri(4-aminophenoxy)triazine.

2,4,6-tris(4-nitrophenoxy)triazine: White crystalline solid; yield 91%; m.p. 208–212 ℃; IR (KBr, ν/cm^{-1}): 1614.40, 1567.46, 1487.24, 1374.32, 1346.28, 1527.10; ^{1}H NMR (400 MHz, $CDCl_3$): δ 8.33 (d, J = 8.76 Hz, 6H, benzene-H), 7.37 (d, J = 9.0 Hz, 6H, benzene-H); ^{13}C NMR (400 MHz, $CDCl_3$):173.07, 162.56, 145.91, 125.55, 122.39.

2,4,6-tri(4-aminophenoxy)triazine: Pale yellow solid; yield 68%; m.p. 225–228 ℃; IR (KBr, ν/cm^{-1}): 3341.45, 1614.44, 1510.22, 1475.14, 1386.27; ^{1}H NMR (400 MHz, $CDCl_3$): δ 6.94 (d, J = 8.76 Hz, 6H, benzene-H), 6.65 (d, J = 8.72 Hz, 6H, benzene-H), 3.70 (s, 6H, $-NH_2$); ^{13}C NMR (400 MHz, $(CD_3)_2SO$): 174.09, 146.88, 142.24, 122.07, 114.64.

Self-assembly of $[Fe^{II}_4L_4]^{8+}$ complex 1

To a stirred solution of 2,4,6-tris(4-aminophenoxy)triazine (25.0 mg, 0.062 mmol) in 10 mL CH_3CN was added 3-methylpyridine 2-formaldehyde (21.9 mg, 0.186 mmol) and iron(II) trifluoromethanesulfonate ($Fe(OTf)_2$, 22.0 mg, 0.062 mmol)(Scheme 3). The mixture was stirred under 30 ℃ for 12 h to give a dark red solution. Then the solution was cooled to room temperature and 10 mL Et_2O was added. The compound of **1** was precipitated and collected by filtration to give a purple red solid. The crude product was purified by recrystallization in acetonitrile.

$[Fe^{II}_4L_4]^{8+}$ complex: purple red solid; yield 58.3%; m.p. > 300 ℃; ^{1}H NMR (400 MHz, CD_3CN): δ 9.00 (s, $3H_e$), 8.11 (d, J = 8.5 Hz, $3H_b$), 7.59 (t, J = 12.9 Hz, $3H_c$), 7.45 (d, J = 7.5 Hz, $3H_h$), 7.18 (d, J = 7.1 Hz, $3H_i$), 7.01 (d, J = 5.0 Hz, $3H_d$), 5.79 (d, J = 9.5 Hz, $3H_g$), 5.18 (d, J = 8.6 Hz, $3H_f$), 2.79 (s, 3H, $9H_a$); Anal Calcd for $C_{176}H_{132}Fe_4N_{36}O_{36}S_8F_{24}$: C, 49.59; H, 3.12; N, 11.83; found: C, 49.08; H, 3.08; N, 12.01; ESI-MS of $[\mathbf{1}\cdot OTf]^{7+}$ for $C_{169}H_{132}Fe_4N_{36}O_{15}SF_3$: m/z 459.83; ESI-MS of $[\mathbf{1}\cdot 2OTf]^{6+}$ for $C_{170}H_{132}Fe_4N_{36}O_{18}S_2F_6$: m/z 561.45; ESI-MS of $[\mathbf{1}\cdot 3OTf]^{5+}$ for $C_{171}H_{132}Fe_4N_{36}O_{21}S_3F_9$: m/z 703.54.

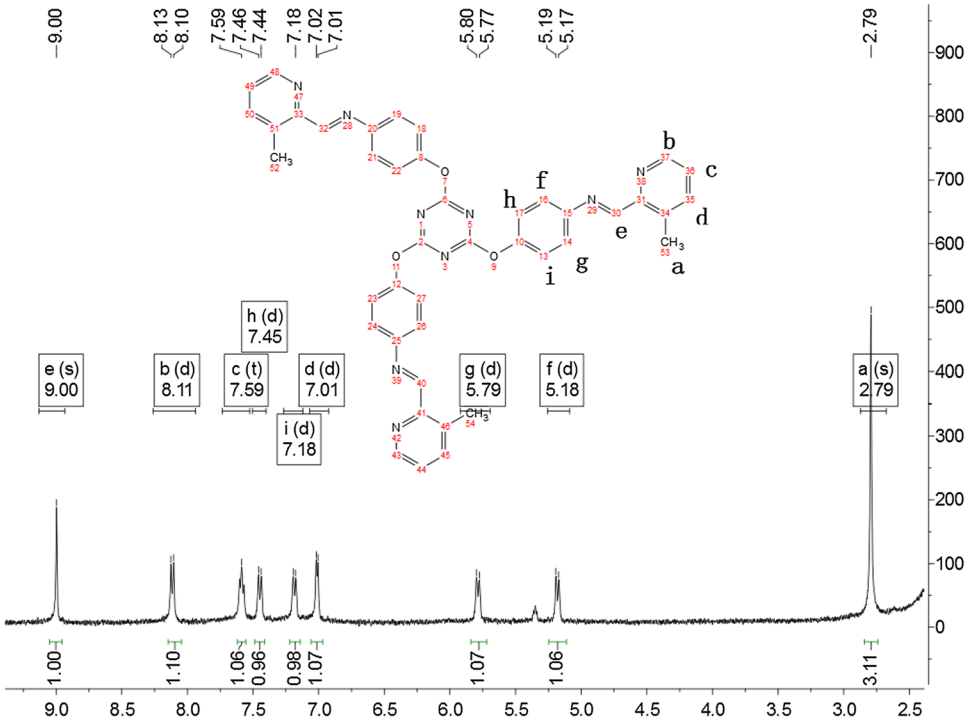

Fig. 1 ^{1}H NMR spectrum of cage **1** in CD_3CN at 293 K

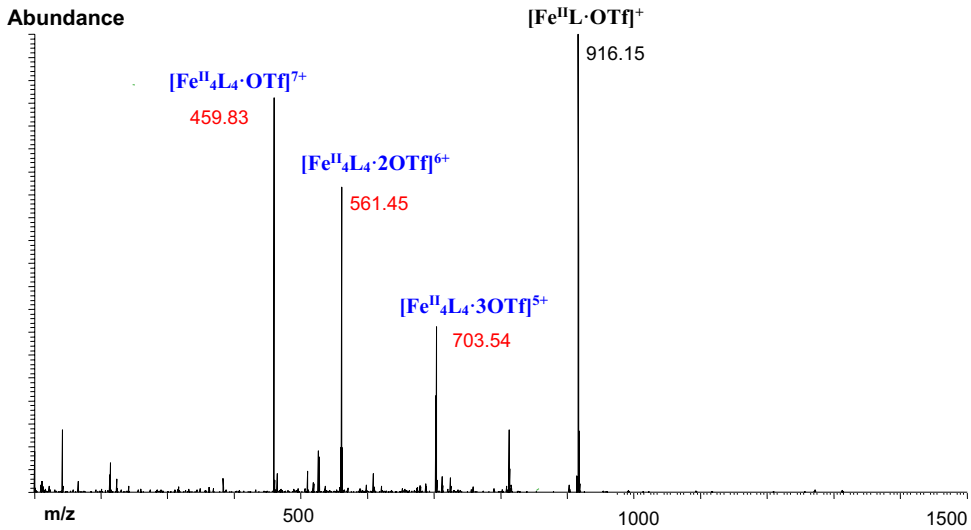

Fig. 2 ESI-MS peaks relative to cage **1** in CH_3CN solution

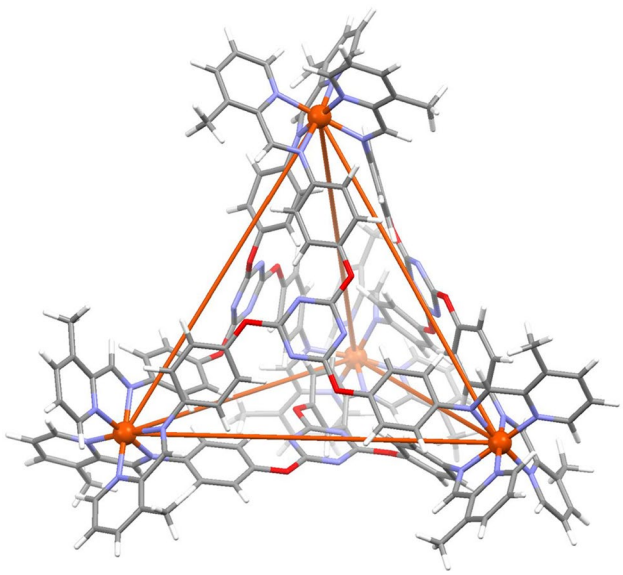

Fig. 3 MM2 model of tetrahedral cage **1**

Results and discussion

Structural features of the tetrahedral cage

The tetrahedral cage **1** was confirmed by ^{1}H NMR and ESI-MS measurements (Figs. 1, 2). The only one set singles of ligand reflects high-symmetrical arrangement of cage **1** and ESI-MS spectrum clearly gives the peaks of the $[Fe^{II}{}_4L_4{\cdot}n(OTf)]^{8-n}$ (n = 1 ~ 3) series. Also the peak of m/z = 916.15 could be assigned to the $[Fe^{II}L{\cdot}OTf]^+$ fragment of cage structure during the ionization process. The isotopic peaks analysis is presented in Fig.S6. As the crystal of **1** suitable for X-ray determination has not been achieved yet, the *MM2* force field model (CAChe Work System Pro 2000–2006) based on the crystal structures of a similar Fe_4L_4 cage series (Ferguson et al. 2014), where different C_3-symmetric triamines and formaldehyde have been applied, was optimized and used to discuss the structure of our complex.

Through the simulation structure of cage **1** (Fig. 3), there are four identical C_3-symmetrical Schiff base ligands capping the four faces of the tetrahedral cage, coordinated by four octahedral Fe(II) ions at the four vertexes of the tetrahedron. Compared with the structure of our formerly reported Fe_2L_3 helicate (Fu et al. 2018), the ether groups added in the ligand not only enlarge the Fe(II)–Fe(II) distance from 11.9 Å in helicate to 14.21–15.69 Å in cage **1**, but also succeed in the preferred cage structure. The single σ bond on both sides of ether group can rotate freely, greatly increasing the spatial freedom of terminal coordination sites in the ligand, which fully meets the coordination configuration of the metal ions during the self-assembly process. Finally the novel tetrahedral cage structure is achieved rather than the much simpler helicate. The volume of the central cavity is calculated to be about 185 $Å^3$ by using VOIDOO program (Kleywegt et al. 1994, Caulder and Raymond 1999b).

The inner core of the complex has the cavity, while along the edges of the tetrahedral cage, there also exist peripheral apertures. Inner cavity and peripheral apertures surely make this tetrahedral cage become adventure land for guest molecules to enter and exit.

^{1}H NMR studies of host–guest chemistry

Six various aromatic guests (Scheme 4) of high symmetry were selected to explore the host–guest ^{1}H NMR investigations. The host cage **1** (0.01 mmol, 1 eq) was dissolved in

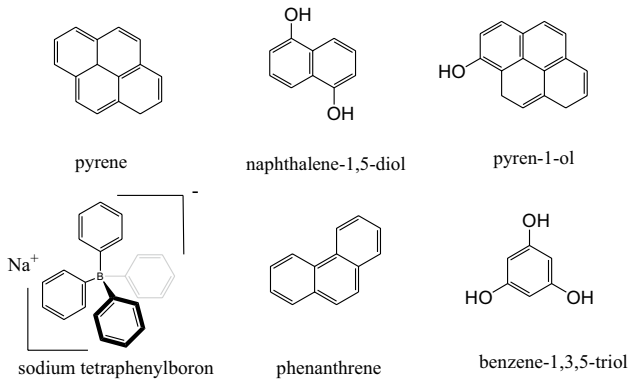

Scheme 4 Guest molecules used in host–guest investigation

1 mL CD_3CN and then one of the chosen guest molecules (0.1 mmol, 10 eq) was added individually. After stirring reaction (at least for 2 h) over, the whole system was analyzed by ^{1}H NMR to obtain the data of host–guest interaction (Figs. S7–S18).

From the ^{1}H NMR spectra, it's observed that with different guest molecules adding, the proton signals of the host and guest molecules have more or less changed. The signals attributed to the excessive guest molecules were kept in one set and had not many change compared with the ^{1}H NMR of free guests ($\Delta\delta < \pm 0.02$ ppm), which declared the rapidly exchange mode between free and possible bound states of guests on the NMR time scale (Ronson et al. 2014).

Based on former knowledge, the host NMR signals' up field shifts are connected with the increasing of electron density in the ligand's conjugated system which could owe to supramolecular interactions such as π–π stacking with the electron-rich guests (Rizzuto et al. 2016). Meanwhile, after adding pyrene molecules into the host solution, the most up field shift ($\Delta\delta = -0.01$ ppm) is very slight, which suggests the weakness of π-π stacking interactions. Other planer neutral aromatic guests all failed in significant field shift in the host ^{1}H signals (Table 1). It could be explained why the π-π stacking could hardly occur in cage **1,** for the insertion of ether group breaks the conjugation system between the triazine core and outstretching phenyl rings. Thus the π-π stacking interactions between host and guest in the formerly reported helicate vanished in the cage **1** system.

The only guest exhibiting moderate host–guest interactions is sodium tetraphenylboron ($NaBPh_4$). The tetraphenylborate is the anion and has extra electronic density while the tetrahedral shape could fit the grooves of similar C_3-symmetric ligands in our formerly reported Zn_3L_2 triangular double helicate **2** (Wu et al. 2018) and then offers the electronic perturbation to nearby hydrogens of the host via C–H…π interactions.

As seen in Fig. 4a, the most up field shifts of ^{1}H signals (H_a and H_c) are from the outward pyridine ring, not involved in the inner phenyl part of the ligand in **1** (H_f, H_g, H_h and H_i). While in Fig. 4b, the most significant changes of ^{1}H signals ($H_{g'}$ and $H_{e'}$) occur to the groove between the outstretched arms of the ligand in **2**. Also the maximum shifts ($\Delta\delta = -0.18 \sim -0.20$ ppm) in **2** are also larger than those in **1** ($\Delta\delta = -0.08$ ppm), which suggests the stronger binding of guests around the groove part of host.

This can be explained with steric hindrance of the methyl groups attached in the pyridine ring of **1**, which interferes the complementary arrangement of tetraphenylborate anions with peripheral apertures formed by the ligand's grooves along the edges of the tetrahedral cage. So the tetraphenylborate guest could only have chance to approach the vertexes of the cage structure, and uses its electron-rich phenyl rings as the acceptors of relative week C–H…π interactions, while H atoms (H_a, H_b, H_c and H_e) from pyridine ring coordinated with positive-charged metal center act as donors.

Table 1 Summary changes of chemical shift value of protons in cage ligand during the host–guest interaction

	Host−only	+Pyrene	+Naphthalene-1,5-diol	+Pyren-1-ol	+$NaBPh_4$	+Phenanthrene	+Benzene-1,3,5-triol
H_a	2.79	2.78 (−0.01)	2.79 (0)	2.78 (−0.01)	2.71 (−0.08)	2.78 (−0.01)	2.78 (−0.01)
H_b	8.11	8.10 (−0.01)	8.10 (−0.01)	Covered**	8.06 (−0.05)	8.11(0)	8.11 (0)
H_c	7.59	7.58 (−0.01)	7.57 (−0.02)	Covered**	7.51 (−0.08)	7.58 (−0.01)	7.58 (−0.01)
H_d	7.01	7.01 (0)	Covered**	7.01 (0)	Covered**	7.01(0)	Covered**
H_e	9.00	8.99 (−0.01)	9.00 (0)	8.99 (−0.01)	8.94 (−0.06)	8.99 (−0.01)	9.00 (0)
H_f	5.18	5.19 (0.01)	5.18 (0)	5.19 (0.01)	5.18 (0)	5.19(0.01)	5.19 (0.01)
H_g	5.79	5.78 (−0.01)	5.79 (0)	5.78 (−0.01)	5.75 (−0.04)	5.78 (−0.01)	5.78 (−0.01)
H_h	7.45	7.46 (0.01)	7.44 (−0.01)	7.45 (0)	7.45 (0)	7.45 (0)	7.44 (−0.01)
H_i	7.18	7.19 (0.01)	7.17 (−0.01)	7.18 (0)	7.13 (−0.05)	7.18 (0)	7.18 (0)

*All signals were calibrated base on the CD_3CN solution peak $\delta = 1.94$ ppm

**Covered = signals covered by the peaks of guest, cannot be recognized clearly

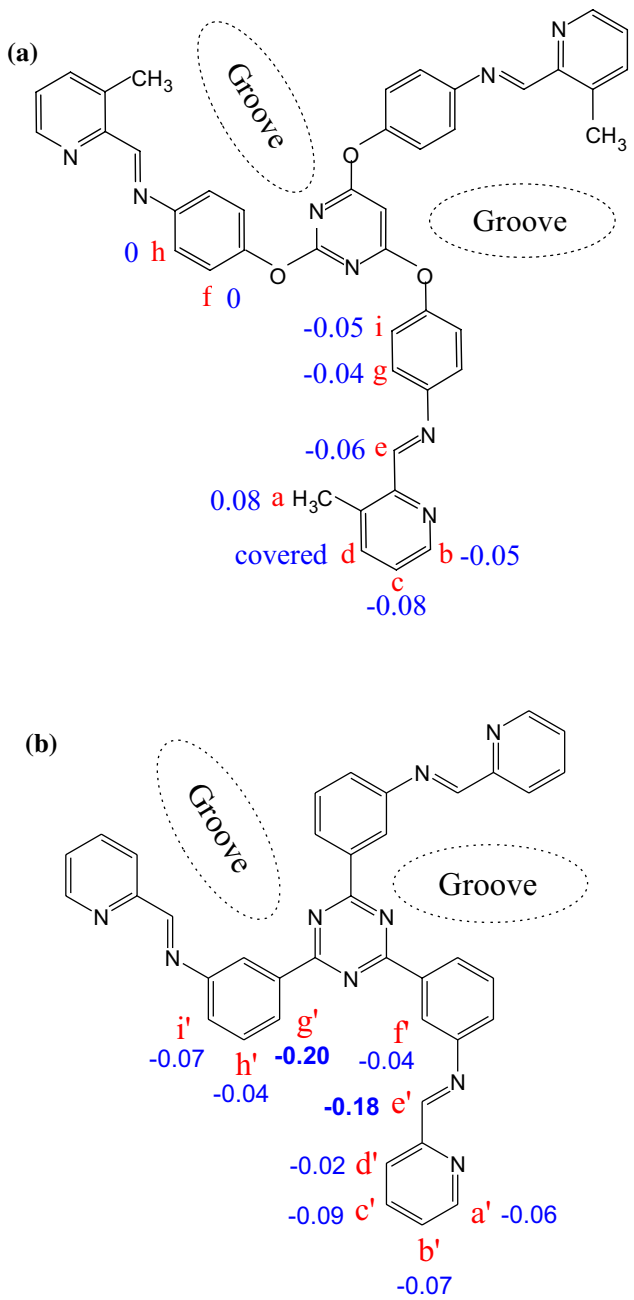

Fig. 4 The host–guest interaction patterns of ligands in **a** cage **1** and **b** helicate **2** with $NaBPh_4$, showing the shift of corresponding ^1H NMR signals

Conclusions

In this paper, a novel metal–organic cage $[Fe^{II}_4L_4]^{8+}$ cage was synthesized by self-assembly of 2, 4, 6-tris (4-aminophenoxy) triazine as subcomponent with 3-methylpyridine-2-carbosaldehyde and iron(II) trifluoromethanesulfonate in CH_3CN solution. The insertion of ether group significantly changes the performance of the designed ligand, and then the tetrahedral structure of this cage complex is confirmed by ^1H NMR and ESI-MS measurements. The host–guest investigations by tracing shifts of host ^1H NMR signals show that non-planar tetraphenylborate anion has moderate influence on the host complex than the planar aromatic guests due to the extra electronic density. And the methyl groups attached in the pyridine ring hinder the relative larger tetraphenylborate anion from further interactions within the peripheral apertures of the cage.

Supplementary Information The online version contains supplementary material available at https://doi.org/10.1007/s11696-021-01685-w.

Acknowledgements This work has been funded by the College Students' Innovation and Open Experimentation Fund Project, NJTECH (2021DC0472 & 2021DC0474).

Declarations

Conflict of interest The authors declare that they have no conflict of interest.

References

Ariga K, Ito H, Hillab JP, Tsukube H (2012) Molecular recognition: from solution science to nano/materials technology. Chem Soc Rev 41:5800–5835. https://doi.org/10.1039/C2CS35162E

Bonnet S, Collin JP, Koizumi M, Mobian P, Sauvage JP (2006) Transition-metal-complexed molecular machine prototypes. Adv Mater 18:1239–1250. https://doi.org/10.1002/adma.200502394

Breiner B, Clegg JK, Nitschke JR (2011) Reactivity modulation in container molecules. Chem Sci 2:51–56

Brenner W, Ronson TK, Nitschke JR (2017) Separation and Selective Formation of Fullerene Adducts within an MII8L6 Cage. J Am Chem Soc 139:75–78. https://doi.org/10.1021/jacs.6b11523

CAChe Work System Pro (2000–2006) Fujitsu Limited, Beaverton, Oregon, Version 7.5.0.85

Castilla AM, Ramsay WJ, Nitschke JR (2014) Stereochemistry in Subcomponent Self-Assembly. Acc Chem Res 47:2063–2073. https://doi.org/10.1021/ar5000924

Caulder DL, Raymond KN (1999a) Supermolecules by Design. Acc Chem Res 32:975–982. https://doi.org/10.1021/ar970224v

Caulder DL, Raymond KN (1999b) The rational design of high symmetry coordination clusters. J Chem Soc Dalton Trans 8:1185–1200. https://doi.org/10.1039/A808370C

Chakrabarty R, Mukherjee PS, Stang PJ (2011) Supramolecular coordination: self-assembly of finite two- and three-dimensional ensembles. Chem Rev 111:6810–6918. https://doi.org/10.1021/cr200077m

Chichak KS, Cantrill SJ, Pease AR, Chiu SH, Cave GWV, Atwood JL, Stoddart JF (2004) Molecular borromean rings. Science 304:1308–1312. https://doi.org/10.1126/science.1096914

Clever GH, Tashiro S, Shionoya M (2009) Inclusion of anionic guests inside a molecular cage with Palladium(II) centers as electrostatic anchors. Angew Chem Int Ed 48:7010–7012. https://doi.org/10.1002/anie.200902717

Cram DJ (1992) Molecular container compounds. Nature 356:29–36. https://doi.org/10.1038/356029a0

Du J-L, Hu T-L, Zhang S-M, Zeng Y-F, Bu X-H (2008) Tuning silver(I) coordination architectures by ligands design: from dinuclear, trinuclear, to 1D and 3D frameworks. Cryst Eng Comm 10:1866–1874. https://doi.org/10.1039/B810773D

Ferguson A, Staniland RW, Fitchett CM, Squire MA, Williamsona BE, Kruger PE (2014) Variation of guest selectivity within [Fe4L4]8+ tetrahedral cages through subtle modification of the face-capping ligand. Dalton Trans 43:14450–14553. https://doi.org/10.1039/C4DT02337D

Fu XH, Wu WY, Jiang P, Han ZY, Wan R (2018) Self-assembly and host-guest behaviors of a supramolecular helicate FeII 2L3. Química Nova 41(5):528–532. https://doi.org/10.21577/0100-4042.20170217

Fujita M, Tominaga M, Hori A, Therrien B (2005) Coordination assemblies from a Pd(II)-cornered square complex. Acc Chem Res 38:369–378. https://doi.org/10.1021/ar040153h

Furutani Y, Kandori H, Kawano M, Nakabayashi K, Yoshizawa M, Fujita M (2009) In situ spectroscopic, electrochemical, and theoretical studies of the photoinduced host−guest electron transfer that precedes unusual host-mediated alkane photooxidation. J Am Chem Soc 131:4764–4768. https://doi.org/10.1021/ja8089075

Gupta S, Choudhury R, Krois D, Brinke UH, Ramamurthy V (2012) Cucurbituril adamantanediazirine complexes and consequential carbene chemistry. J Org Chem 77:5155–5160. https://doi.org/10.1021/jo300571p

Hasenknopf B, Lehn JM, Kneisel BO, Baum G, Fenske D (1996) Selbstaufbau eines zirkularen Doppelhelicates. Angew Chem Int Ed 108:987–1990. https://doi.org/10.1002/ange.19961081632

Horiuchi S, Murase T, Fujita M (2011) Noncovalent trapping and stabilization of dinuclear ruthenium complexes within a coordination cage. J Am Chem Soc 133:12445–12447. https://doi.org/10.1021/ja205450a

Kleywegt GJ, Jones TA (1994) Detection, delineation, measurement and display of cavities in macromolecular structures. Acta Crystallogr Sect D 50:178–185. https://doi.org/10.1107/S0907444993011333

Li Y-P, Yang H-R, Zhao Q, Song W-C, Han J, Bu X-H (2012) Ratiometric and selective fluorescent sensor for Zn2+ as an "Off–On–Off" switch and logic gate. Inorg Chem 51:9642–9648. https://doi.org/10.1021/ic300738e

Li ZY, Dai JW, Damjanović M, Shiga T, Wang JH, Zhao J, Oshio H, Yamashita M, Bu XH (2019) Structure switching and modulation of the magnetic properties in diarylethene-bridged metallosupramolecular compounds by controlled coordination-driven self-assembly. Angew Chem Int Ed 58(13):4339–4344. https://doi.org/10.1002/anie.201900789

Liu C-S, Chen P-Q, Yang E-C, Tian J-L, Bu X-H, Li Z-M, Sun H-W, Lin Z-Y (2006) Silver(I) complexes in coordination supramolecular system with bulky acridine-based ligands: syntheses, crystal structures, and theoretical investigations on C−H·Ag Close interaction. Inorg Chem 45:5812–5821. https://doi.org/10.1021/ic060087a

Murase T, Horiuchi S, Fujita M (2010) Naphthalene Diels−Alder in a self-assembled molecular flask. J Am Chem Soc 132:2866–2867. https://doi.org/10.1021/ja9107275

Nakabayashi K, Ozaki Y, Kawano M, Fujita M (2008) A self-assembled spin cage. Angew Chem Int Ed 47:2046–2048. https://doi.org/10.1002/anie.200704924

Neelakandan PP, Jiménez A, Thoburn JD, Nitschke JR (2015) An autocatalytic system of photooxidation-driven substitution reactions on a FeII4L6 cage framework. Angew Chem Int Ed 54:14378–14382. https://doi.org/10.1002/anie.201507045

Riddell IA, Smulders MMJ, Clegg JK, Nitschke JR (2011) Encapsulation, storage and controlled release of sulfur hexafluoride from a metal–organic capsule. Chem Commun 47:457–459. https://doi.org/10.1039/C0CC02573A

Rizzuto FJ, Wu W-Y, Ronson TK, Nitschke JR (2016) Peripheral templation generates an MII6L4 guest-binding capsule. Angew Chem Int Ed 55:7958–7962. https://doi.org/10.1002/anie.201602135

Ronson TK, Zarra S, Black SP, Nitschke JR (2013) Metal–organic container molecules through subcomponent self-assembly. Chem Commun 49:2476–2490. https://doi.org/10.1039/C2CC36363A

Ronson TK, League AB, Gagliardi L, Cramer CJ, Nitschke JR (2014) Pyrene-edged FeII4L6 cages adaptively reconfigure during guest binding. J Am Chem Soc 136:15615–15624. https://doi.org/10.1021/ja507617h

Schneider MW, Hauswald HJS, Stoll R, Mastalerz M (2012) A shape-persistent exo-functionalized [4 + 6] iminecage compound with a very high specific surface area. Chem Commun 48:9861–9863. https://doi.org/10.1039/C2CC35002E

Sun Q-F, Iwasa J, Ogawa D, IshidoY SS, Ozeki T, Sei Y, Yamaguchi K, Fujita M (2010) Self-Assembled M24L48 Polyhedra and Their Sharp Structural Switch upon Subtle Ligand Variation. Science 328:1144–1147. https://doi.org/10.1126/science.1188605

Wu W-Y, Fu X-H, Jiang P, Tang T-H, Li W-Z, Wan R (2018) Self-assembly and peripheral guest-binding of [Zn3L2(H2O)6]6 + triangular double helicate. Inorg Chem Commun 89:1–4. https://doi.org/10.1016/j.inoche.2017.12.017

Yoshizawa M, Kumazawa K, Fujita M (2005) Room-Temperature and solution-state observation of the mixed-valence cation radical dimer of tetrathiafulvalene, [(TTF)2]+•, within a self-assembled cage. J Am Chem Soc 127:13456–13457. https://doi.org/10.1021/ja053508g

Yu M-H, Liu X-T, Space B, Chang Z, Bu X-H (2021) Metal-organic materials with triazine-based ligands: from structures to properties and applications. Coord Chem Rev 427:213518–213562. https://doi.org/10.1016/j.ccr.2020.213518

Zarra S, Wood DM, Roberts DA, Nitschke JR (2015) Molecular containers in complex chemical systems. Chem Soc Rev 44:419–432. https://doi.org/10.1039/C4CS00165F

Publisher's Note Springer Nature remains neutral with regard to jurisdictional claims in published maps and institutional affiliations.